Molecular Biology of the Cell
Vol. 15, 3938–3949, August 2004

Inositol 1,4,5-Trisphosphate Signaling Regulates Rhythmic Contractile Activity of Myoepithelial Sheath Cells in *Caenorhabditis elegans*

Xiaoyan Yin,* Nicholas J.D. Gower,† Howard A. Baylis,† and Kevin Strange*‡

*Departments of Anesthesiology, Molecular Physiology and Biophysics, and Pharmacology, Vanderbilt University Medical Center, Nashville, Tennessee 37232; and †Department of Zoology, University of Cambridge, Cambridge, United Kingdom CB2 3EJ

Submitted March 10, 2004; Revised May 24, 2004; Accepted May 30, 2004
Monitoring Editor: Susan Strome

Intercellular communication between germ cells and neighboring somatic cells is essential for reproduction. *Caenorhabditis elegans* oocytes are surrounded by and coupled via gap junctions to smooth muscle-like myoepithelial sheath cells. Rhythmic sheath cell contraction drives ovulation and is triggered by a factor secreted from oocytes undergoing meiotic maturation. We demonstrate for the first time that signaling through the epidermal growth factor-like ligand LIN-3 and the LET-23 tyrosine kinase receptor induces ovulatory contractions of sheath cells. Reduction-of-function mutations in the inositol 1,4,5-trisphosphate (IP_3) receptor gene *itr-1* and knockdown of *itr-1* expression by RNA interference inhibit sheath contractile activity. *itr-1* gain-of-function mutations increase the rate and force of basal contractions and induce tonic sheath contraction during ovulation. Sheath contractile activity is disrupted by RNAi of *plc-3*, one of six phospholipase C-encoding genes in the *C. elegans* genome. PLC-3 is a PLC-γ homolog and is expressed in contractile sheath cells of the proximal gonad. Maintenance of sheath contractile activity requires plasma membrane Ca^{2+} entry. We conclude that IP_3 generated by LET-23 mediated activation of PLC-γ induces repetitive intracellular Ca^{2+} release that drives rhythmic sheath cell contraction. Calcium entry may function to trigger Ca^{2+} release via IP_3 receptors and/or refill intracellular Ca^{2+} stores.

INTRODUCTION

Communication between developing germ cells and surrounding somatic cells is essential for reproduction (Cheng and Mruk, 2002; Eppig, 2001; Matzuk *et al.*, 2002). The *Caenorhabditis elegans* gonad is a powerful model system in which to define the molecular bases of these communication processes (Hubbard and Greenstein, 2000). Adult *C. elegans* hermaphrodites possess two U-shaped gonad arms connected via spermathecae to a common uterus. Oocytes form in the proximal gonad and accumulate in a single-file row of graded developmental stages. Developing oocytes remain in diakinesis of prophase I until they reach the most proximal position in the gonad arm where they undergo meiotic maturation and are then ovulated into the spermatheca for fertilization (reviewed by Hubbard and Greenstein, 2000).

Oocytes are surrounded by and coupled via gap junctions to myoepithelial sheath cells (Hall *et al.*, 1999). Before ovulation, sheath cells contract weakly at a basal rate of seven to eight contractions per minute (McCarter *et al.*, 1999). Basal sheath contractions are triggered by release of major sperm protein (MSP) from sperm stored in the spermatheca (Miller *et al.*, 2001). MSP also triggers meiotic maturation in the most proximally located oocyte (Miller *et al.*, 2001). A signal released from the maturing oocyte induces ovulation by increasing the rate and force of sheath cell contractions and triggering spermatheca dilation (Iwasaki *et al.*, 1996; McCarter *et al.*, 1999).

clh-3 encodes a voltage-gated ClC anion channel (Rutledge *et al.*, 2001; Rutledge *et al.*, 2002). A CLH-3 splice variant, CLH-3b, is expressed in *C. elegans* oocytes and is activated during meiotic maturation by serine/threonine dephosphorylation events (Denton *et al.*, 2003). Disruption of *clh-3* expression by RNA interference (RNAi) (Rutledge *et al.*, 2001) or deletion mutagenesis (Yin and Strange, unpublished observations) causes early onset of ovulatory sheath cell contractions, indicating that CLH-3b functions normally to inhibit sheath contractility (Rutledge *et al.*, 2002; Strange, 2003). Expression of *clh-3* has not been detected in sheath cells (Schriever *et al.*, 1999; Nehrke *et al.*, 2000; Denton *et al.*, 2003), suggesting that sheath contractility is modulated by channel activity in the oocyte.

Maturation-induced activation of CLH-3b depolarizes the oocyte and most likely the gap junction-coupled sheath cells. We postulated that this depolarization in turn inhibits sheath cell Ca^{2+} influx required for generating and/or maintaining inositol 1,4,5-trisphosphate (IP_3)-dependent release of Ca^{2+} from intracellular stores (Rutledge *et al.*, 2002; Strange, 2003). To begin testing this hypothesis, we examined the role of IP_3 signaling pathways in regulating sheath cell contraction. Genetic analyses have shown clearly that

Article published online ahead of print. Mol. Biol. Cell 10.1091/mbc.E04–03–0198. Article and publication date are available at www.molbiolcell.org/cgi/doi/10.1091/mbc.E04–03–0198.

‡ Corresponding author. E-mail address: kevin.strange@vanderbilt.edu.

[1] *pll*-1 is the *C. elegans* homologue of mammalian PLC-like proteins that are catalytically inactive (Kanematsu *et al.*, 1996; Otsuki *et al.*, 1999). A histidine residue critical for phospholipase activity is mutated in these proteins. The same mutation is present in PLL-1, suggesting that is also catalytically inactive.

IP_3 signaling plays a central role in regulating spermatheca dilation, which is required for successful ovulation (Clandinin *et al.*, 1998; Bui and Sternberg, 2002). However, the intracellular signaling pathways controlling sheath cell contraction are unknown. We demonstrate here for the first time that IP_3 regulates both basal and ovulatory contractile activity in *C. elegans* sheath cells. IP_3 is generated by PLC-γ, which is activated by signaling through LIN-3/LET-23 and MSP/VAB-1.

MATERIALS AND METHODS

C. elegans Strains

Nematodes were cultured using standard methods (Brenner, 1974). Wild-type worms were the Bristol N2 strain. The following alleles were used: *itr-1(sa73, sy327), unc-24(e138), fog-2(q71), rrf-1(pk1417), lin-3(n1058), let-23(sy10), unc-4(e120). itr-1(sa73)* is a temperature-sensitive allele, and worms harboring this mutation were grown at the semipermissive temperature of 20°C. All other strains were grown at 16–25°C.

In Vivo and In Vitro Analysis of Sheath Contraction and Ovulation

Adult worms (2–4 d old) were anesthetized in M9 solution containing 0.1% tricaine and 0.01% tetramisole for 20–40 min and then mounted onto 2% agarose pads (McCarter *et al.*, 1999). Worms were imaged at room temperature (22–23°C) by differential interference contrast microscopy by using a Nikon (Melville, NY) Eclipse TE2000 inverted microscope and a Plan Apo 60× (1.4 numerical aperture) oil immersion objective lens. Images were recorded at 30 frames/s on videotape by using a Dage-MTI (Michigan City, IN) charge-coupled device 100 camera and analyzed offline. Sheath contractions were counted in 1-min intervals. The intensity or force of individual contractions was estimated by measuring lateral displacement of the sheath as described previously (Miller *et al.*, 2001).

Single nematodes were placed in saline (161 mM NaCl, 5 mM KCl, 2 mM $CaCl_2$, 2 mM $MgCl_2$, 25 mM HEPES, pH 7.3, 340–350 mOsM), and gonads were isolated by cutting them behind the pharyngeal bulb and in front of the spermatheca using a 26-gauge needle. Isolated gonads were transferred to a bath chamber (model R-26G; Warner Instruments, Hamden, CT) with a poly-L-lysine–coated glass coverslip bottom. Gonads were imaged at 30×, and rates of sheath contraction determined as described above.

Brood Assay

Brood size was quantified by transferring L4 larvae to clean plates every 24 h for 4 d. The number of progeny on each plate was counted 2 d after eggs hatched.

Synthesis and Injection of Major Sperm Protein Carboxy Terminus (MSP-CT) Peptide

The MSP-CT peptide REWFQGDGMVRRKNLPIEYNP was synthesized by Sigma-Aldrich (St. Louis, MO). Water or 80 nM MSP-CT dissolved in water was injected into the uterus via the vulval opening by glass micropipette. Injected worms were allowed to recover for 30–90 min and then prepared for imaging as described above.

RNA Interference

RNAi was induced by feeding worms bacteria producing double stranded RNA (dsRNA) to target genes (Kamath *et al.*, 2000). Briefly, cDNA encoding regions of the target gene were obtained by polymerase chain reaction (PCR) by using an oligo dt-primed cDNA library (kindly provided by Dr. Robert Barstead, Oklahoma Medical Research Foundation). cDNAs were inserted into vector pPD129.36 by using *Kpn*I and *Xba*I restriction sites flanked by T7 RNA polymerase promoters. pPD128.110, a derivative of pPD129.36 containing a green fluorescent protein (GFP) cDNA, was used as a control in all feeding experiments. HT115(DE3) *Escherichia coli* were transformed with engineered vectors and fed to worms as described previously (Kamath *et al.*, 2000). The location of cDNAs used for each gene studied were as follows: *itr-1*, 427-1241 base pairs; *egl-8*, 1853–2721 base pairs; *plc-1*, 325-1323 base pairs; *plc-3*, 1946–3018 base pairs; *plc-2*, 362-1447 base pairs; *pll-1*, 1430–2368 base pairs; *plc-4*, 1312–2219 base pairs; *lin-3*, 150-1052 base pairs; *vab-1*, 1321–2190 base pairs; and *let-23*, 1571–2650 base pairs.

Construction of Transgenes and Transgenic Worms

The IP_3 binding domain of *itr-1* (residues 1–705) was used as an IP_3 chelator or "sponge" as described previously (Walker *et al.*, 2002). Expression of the IP_3 sponge or GFP in sheath cells was driven by a 6.7-kb sequence upstream of the *let-502* start codon. This sequence was cut from cosmid C10H11 by using flanking *Sph*I and *Pst*I restriction sites. The IP_3 sponge and GFP cDNAs were amplified from pGLB350 (Walker *et al.*, 2002) and pPD95.75 (www.ciwemb.edu/pub/FireLabInfo/FireLabVectors) by using primers containing *Pst*I and *Not*I restriction sites. A new vector designated pXYY2003.2 was engineered from pPD95.75 by cutting out the GFP fragment by using *Pst*I and *Eco*RI restriction sites and inserting a linker containing a *Not*I restriction site between *Pst*I and *Eco*RI. The *let-502* promoter and IP_3 sponge or GFP were inserted into this new vector sequentially.

Translational fusions of *plc-1* and *plc-3* to GFP were made using a PCR fusion-based method (Hobert, 2002). Briefly, genomic fragments of the *plc-1* and *plc-3* genes were amplified using PCR from *C. elegans* N2 genomic DNA. The reverse oligonucleotide contained a sequence that overlapped with the 5′ end of the GFP gene as contained in pHAB200 (Baylis *et al.*, 1999). These PCR products were then combined with a fragment amplified from pHAB200 containing GFP and the 3′-untranslated region and downstream sequences of *let-858*. The *plc-1* fusion extended 4 kb upstream to exon 17 and the *plc-3* fusion extended 3.4 kb upstream to exon 8. Transgenic worms were generated by DNA microinjection as described by Mello *et al.* (1991) by using *rol-6* as a transformation marker.

Statistical Analysis

Data are presented as means ± SE. Statistical significance was determined using Student's two-tailed *t* test for unpaired means. When comparing three or more groups, statistical significance was determined by one-way analysis of variance. p values of ≤ 0.05 were taken to indicate statistical significance.

RESULTS

IP_3 Receptor Function Is Required for Normal Sheath Cell Contractile Activity

Figure 1A shows a sheath ovulatory contractile cycle in wild-type worms. Under basal conditions, sheath cells contract at a mean rate of eight contractions per minute with a mean displacement of 2.2 μm (Figure 1, B and C). During ovulation, sheath contraction increased to a peak rate of 22 contractions/min and the contractions became more forceful, which was observed as an increase in mean displacement to 4.3 μm (Figure 1, B and C).

A single gene, *itr-1*, encodes the IP_3 receptor (IP_3R) in *C. elegans* (Baylis *et al.*, 1999). ITR-1 is expressed in numerous tissues and cell types, including gonadal sheath cells (Baylis *et al.*, 1999; Dal Santo *et al.*, 1999). To determine whether IP_3 signaling is important in regulating sheath cell contractions, we characterized contractility in *itr*-1 mutant worms. *itr-1(sa73)* is a temperature-sensitive reduction-of-function allele (Iwasaki *et al.*, 1995). Sheath contractility in *itr-1(sa73)* mutants was substantially reduced when worms were grown at the semipermissive temperature of 20°C (Figure 1A). Mean basal and peak sheath contraction rates were 1.5 contractions/min and 5.1 contractions/min (Figure 1B). Both basal and peak rates of sheath contraction were significantly ($p < 0.0001$) lower than those observed in wild-type animals. However, the force of sheath contraction was similar in wild-type and *itr-1(sa73)* mutants. Mean displacement of the sheath in *itr-1(sa73)* mutants was 1.9 μm under basal conditions and 4.2 μm during peak ovulatory contractions (Figure 1C).

As reported previously (Bui and Sternberg, 2002), ovulation in *itr-1(sa73)* mutants is defective. The distal spermatheca of these worms dilated and constricted multiple times during ovulation. During most ovulation attempts, the spermatheca constricted around the partially ovulated oocyte causing it to tear. Intact or partial oocytes remaining in the gonad typically triggered a second cycle of ovulatory contractions 7–10 min after the first cycle was complete (our unpublished data).

itr-1(sy327) is a gain-of-function *itr-1* allele (Clandinin *et al.*, 1998). Sheath cell contractile activity in *itr-1(sy327);unc-24(e138)* worms was increased compared with *unc-24(e138)* control worms (Figure 2), which behaved similarly to N2 animals. Under basal conditions, sheath cells of *itr-1(sy327)* mutants contracted at a significantly ($p < 0.0001$) higher rate

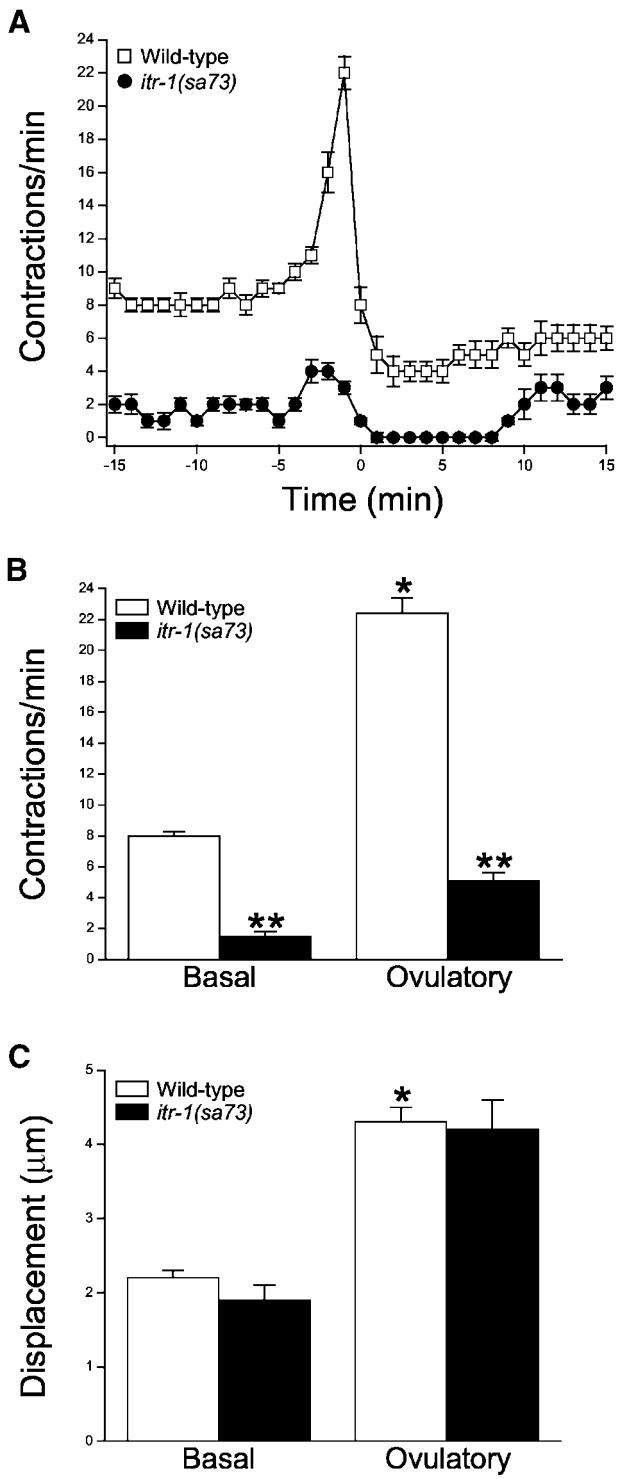

Figure 1. Sheath cell contractions in wild-type and *itr-1(sa73)* mutant worms. (A) Rates of sheath contraction during a single ovulatory cycle. Time 0 in wild-type worms is defined as the time ovulation was completed. In *itr-1(sa73)* mutants, ovulation frequently failed. Therefore, time 0 is defined as the end of forceful ovulatory sheath contractions. Values are means ± SE (n = 11–12). (B and C) Sheath cell contraction rate and displacement under basal conditions and during ovulation in wild-type worms and *sa73* mutants. Ovulatory contraction rate is the peak rate observed. Values are means ± SE (n = 5–11). *$p < 0.0001$ compared with wild-type basal contractions or displacement. **$p < 0.0001$ compared with wild-type.

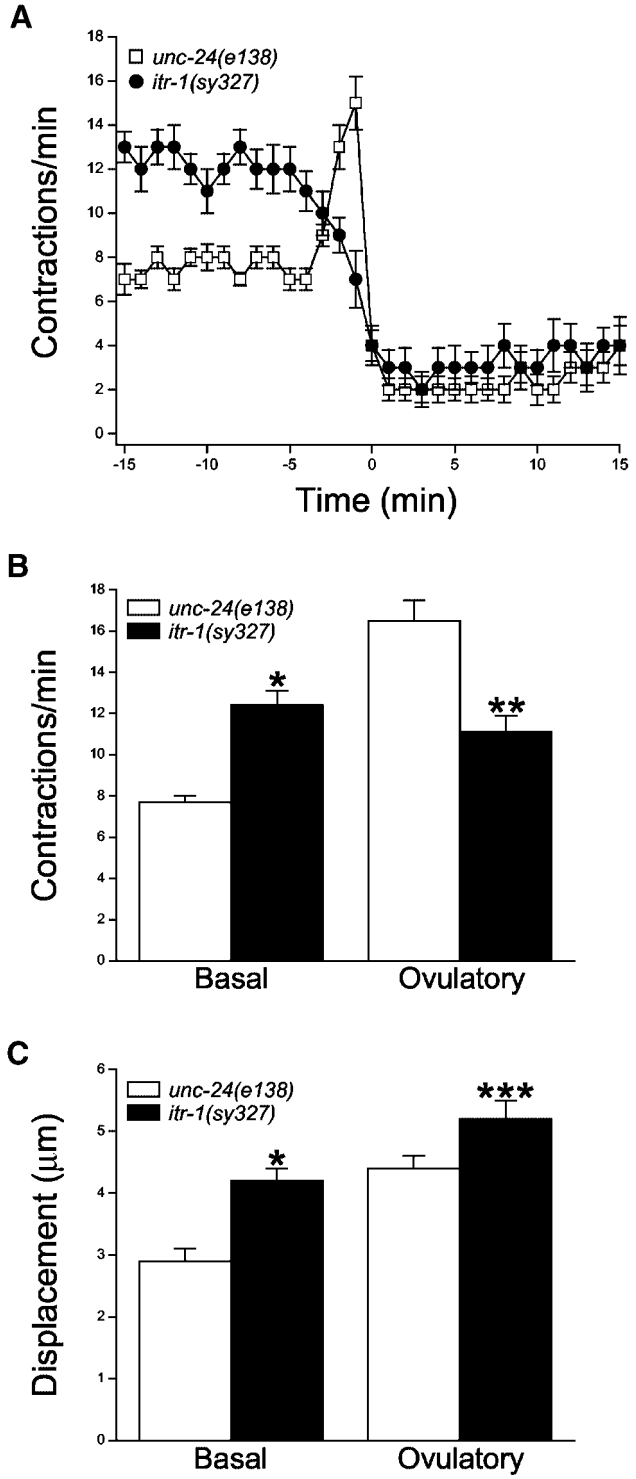

Figure 2. Sheath cell contractions in *unc-24(e138)* control worms and *itr-1(sy327);unc-24(e138)* mutants. (A) Rates of sheath contraction during a single ovulatory cycle. Time 0 is defined as the time ovulation was completed. Values are means ± SE (n = 11–13). (B and C) Sheath cell contraction rate and displacement under basal conditions and during ovulation in control and *itr-1(sy327)* mutants. Ovulatory contraction rate in control worms is the peak rate observed. In *itr-1(sy327)* worms, ovulatory contraction rate was defined as the maximal rate observed between –3 and –1 min. Values are means ± SE (n = 11–14). *$p < 0.0001$ compared with control basal contractions or displacement. **$p < 0.0005$ compared with control ovulatory contractions. ***$p < 0.04$ compared with control displacement.

of 12.4 contractions/min versus 7.7 contractions/min in *unc-24(e138)* control worms (Figure 2B). The basal sheath contractions were also significantly ($p < 0.0001$) more forceful. Mean basal sheath displacements in *unc-24(e138)* worms and *itr-1(sy327)* mutants were 2.9 and 4.2 μm, respectively (Figure 2C).

During ovulation, sheath contractions increased to a peak rate of 16.5 contractions/min in *unc-24(e138)* control worms (Figure 2B). Interestingly, the sheath contraction rate in *itr-1(sy327)* mutants did not increase, but instead declined throughout ovulation (Figure 2A). The mean maximal rate of contraction observed between –3 and –1 min was 11.1 contractions/min, which was significantly ($p < 0.0005$) less than that observed in control animals (Figure 2B). *sy327* ovulatory contractions also seemed to be somewhat more forceful. Mean sheath displacement during ovulation was 5.2 μm in *itr-1(sy327)* mutants, which was significantly ($p < 0.04$) different from a mean value of 4.4 μm observed in control animals (Figure 2C).

In addition to increases in contraction rate and displacement, sheath cells of *itr-1(sy327)* mutants exhibited other characteristics indicative of enhanced contractile activity. We observed that larger segments of the sheath in *itr-1(sy327)* worms were actively contracting during each contraction/relaxation cycle. To quantify this, we measured the distance over which single sheath contraction/relaxation cycles were observed. In *unc-24(e138)* control worms, the mean ± SE contracting sheath length was 13.4 ± 0.9 μm ($n = 10$) under basal conditions and 11.7 ± 1.3 μm ($n = 11$) during ovulation. This length was almost twofold greater in *itr-1(sy327)* mutants. Mean ± SE basal and ovulatory contracting sheath lengths were 25.3 ± 5.7 μm ($n = 11$) and 23.1 ± 2.0 μm ($n = 12$), respectively. Both values were significantly ($p < 0.003$) different from those of control worms.

During ovulation, the sheath of *itr-1(sy327)* mutants seemed to be almost tonically contracted, suggesting that the duration of each sheath contraction was increased compared with control animals. To quantify this, we measured the duration of single contractions, which we defined as the time between the beginning of a contraction and the beginning of the subsequent relaxation. The mean ± SE duration of individual ovulatory contractions in control worms was 1.5 ± 0.04 s ($n = 11$). In *itr-1(sy327)* mutants, the duration of single ovulatory contractions was increased almost threefold to 4.1 ± 0.3 s ($n = 12$). This value was significantly ($p < 0.0001$) different from that observed in control worms. The apparent decrease in the rate of sheath contraction during ovulation (Figure 2A) is likely due to the increased duration of single contractile events.

As a final test for the involvement of IP_3 signaling in sheath contraction, we used an RNAi feeding protocol (Kamath *et al.*, 2000) to disrupt *itr-1* expression. Adult worms fed bacteria producing *itr-1* dsRNA beginning at the L1 larval stage (i.e., long-term feeding) exhibited a severe phenotype. These animals were thin, constipated, sterile, and their gonads contained multiple endomitotic (emo) oocytes. No ovulations were detected in these animals. As shown in Figure 3A, the mean basal sheath contraction rate in *itr-1(RNAi)* worms was 0.4 contractions/min. This value was significantly ($p < 0.0001$) different from the mean basal sheath contraction rate of 7.3 contractions/min observed in control worms fed GFP dsRNA (Figure 3A).

Reduced sheath contractility in worms exposed to long-term *itr-1(RNAi)* could be a secondary consequence of the numerous other defects we observed in these animals. We therefore fed late-stage L4 larvae with dsRNA for 16–24 h

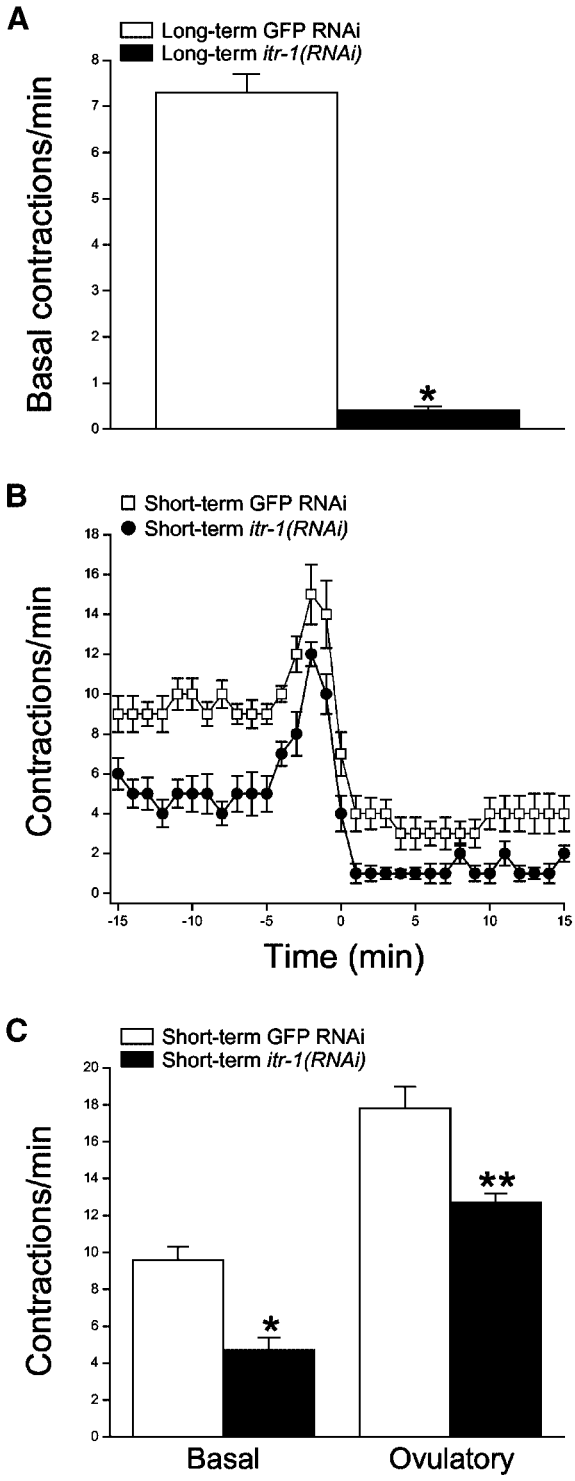

Figure 3. Effect of *itr-1* RNAi expression on sheath contractility. (A) Rates of basal sheath contraction in adult worms fed GFP or *itr-1* dsRNA beginning at the L1 larval stage. Values are means ± SE ($n = 7–11$). *$p < 0.0001$ compared with GFP RNAi worms. (B) Rates of sheath contraction during a single ovulatory cycle. Late-stage L4 larvae were fed dsRNA for 16–24 h. Time 0 is defined as the time ovulation was completed. Values are means ± SE ($n = 10–13$). (C) Basal and peak ovulatory contraction rates. Late-stage L4 larvae were fed dsRNA for 16–24 h. Values are means ± SE ($n = 9–11$). *$p < 0.0001$ and **$p < 0.002$ compared with GFP RNAi worms.

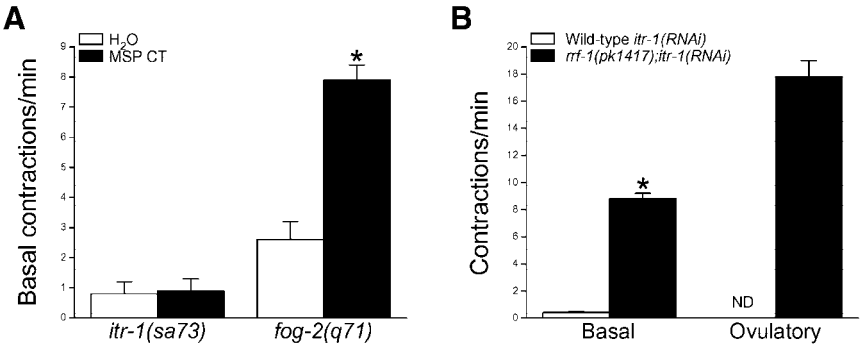

Figure 4. Effects of MSP injection and *itr-1* RNAi in *rrf-1(pk1417)* worms on sheath contractility. (A) Rates of basal sheath contraction in *itr-1(sa73)* and *fog-2(q71)* mutant worms after injection of water or an MSP C-terminal peptide (MSP CT) into the uterus via the vulva. Values are means ± SE (n = 11–17). *$p < 0.0001$ compared with water injected *fog-2(q71)* worms. (B) Basal and peak ovulatory contraction rates in wild-type and *rrf-1(pk1417)* worms fed *itr-1* dsRNA beginning at the L1 larval stage. Ovulatory contractions were not detected in wild-type RNAi worms. Values are means ± SE (n = 4–11). *$p < 0.001$ compared with wild type.

(i.e., short-term feeding). Worms exposed to short-term *itr-1* dsRNA feeding seemed to be healthy and had a largely normal appearance. As shown in Figure 3B, both basal and ovulatory sheath contractions were reduced in these animals compared with control GFP RNAi worms. Mean rates of basal and peak ovulatory contractions were 4.7 and 12.7 contractions/min in *itr-1(RNAi)* worms (Figure 3C). These values were significantly ($p < 0.002$) different from the mean basal and peak ovulatory contraction rates of 9.6 and 17.8 contractions/min observed in control worms (Figure 3C). Together, the data in Figures 1–3 demonstrate that IP_3 signaling regulates sheath cell contraction under basal conditions and during ovulation.

Sheath Cell Contractility Is Not Regulated by IP_3 Signaling in Sperm or Oocytes

Sheath cell contractility is regulated by signals released from germ cells. Basal sheath cell contractions and oocyte meiotic maturation are triggered by MSP secreted from sperm (Miller *et al.*, 2001). Ovulatory sheath cell contractions are triggered by a factor produced by the maturing oocytes (Iwasaki *et al.*, 1996; McCarter *et al.*, 1999). IP_3 signaling regulates secretion in numerous organisms and cell types (Berridge *et al.*, 2000). It is therefore conceivable that the defects in sheath cell contractility shown in Figures 1–3 are due to disruption of sperm and oocyte IP_3 signaling that regulates secretion of sheath contractile factors. We carried out three sets of experiments to test this possibility.

An MSP CT peptide induces basal sheath cell contractions when microinjected into the uterus of sperm-deficient *fog-2* worms (Miller *et al.*, 2001). To determine whether reduced basal sheath contractility observed in *itr-1(sa73)* mutants is due to disrupted MSP secretion, we injected these animals with either MSP CT in water or water alone. Injection of MSP CT into *fog-2* worms increased the rate of basal sheath contraction significantly ($p < 0.0001$) from 2.6 contractions/min to 7.9 contractions/min (Figure 4A). In contrast, MSP CT had no significant ($p > 0.9$) effect on basal sheath contractility in *itr-1(sa73)* reduction-of-function mutants (Figure 4A) demonstrating that MSP signaling in the sheath cells requires functional IP_3 receptors.

Somatic cells of *rrf-1(pk1417)* mutant worms are resistant to dsRNA, but their germline shows an apparently normal RNAi response (Sijen *et al.*, 2001). We fed wild-type and *rrf-1(pk1417)* L1 larvae *itr-1* dsRNA and analyzed sheath contractility in young adults. As noted above, wild-type worms exhibited a severe phenotype. The gonads of all of the worms analyzed (n = 24) contained multiple endomitotic oocytes. In contrast, the gonads of *rrf-1(pk1417);itr-1(RNAi)* mutants were largely normal. Only one or two endomitotic oocytes were detected in 6% of the *rrf-1(pk1417)* mutants examined (n = 33); all other worms had normal oocytes.

Basal and ovulatory sheath contractions in *rrf-1(pk1417); itr-1(RNAi)* mutants (Figure 4B) were similar to those of wild-type control worms (Figure 1). Mean basal and peak ovulatory rates of sheath contraction were 8.8 and 17.8 contractions/min. In contrast, basal sheath contraction rate in wild-type *itr-1(RNAi)* worms was 0.4 contractions/min, and ovulatory contractions were not detected (Figure 4B). These results suggest that the sheath contractility defects observed in wild-type *itr-1(RNAi)* worms are due to disruption of IP_3 signaling in sheath cells rather than in germ cells responsible for secreting factors that regulate contractions.

The N-terminal IP_3 binding domain of *itr-1* can disrupt normal IP_3 signaling by acting as an IP_3 chelator or sponge (Walker *et al.*, 2002). As a final test for the role IP_3 signaling in sheath cells, we generated IP_3 sponge and GFP transgenes under the control of the *let-502* promoter. Figure 5A demonstrates that P*let-502* drives gene expression in sheath cells and the spermatheca. No GFP was detected in sperm or oocytes, which typically do not express transgenes introduced by microinjection due to the formation of multicopy extrachromosomal arrays (Kelly and Fire, 1998).

Three P*let-502*::IP_3 sponge transgenic lines were generated. All of the lines exhibited an emo phenotype. In each line, we examined gonad morphology in 30–49 worms and found that 67–70% of the animals had gonads that contained multiple endomitotic oocytes. Because normal ovulatory behavior cannot be observed in severely emo animals, we quantified sheath contractility in transgenic worms with normal oocytes. As shown in Figure 5, B and C, both basal and ovulatory sheath cell contractions were reduced in P*let-502*::IP_3 sponge worms. Mean basal and peak ovulatory sheath contraction rates were 3.0 and 11.5 contractions/min (Figure 5C). These values were significantly ($p < 0.0002$) less than the mean basal and peak ovulatory contraction rates of 7.8 and 17.1 contractions/min observed in control P*let-502*::GFP worms (Figure 5C). Together, the data in Figures 4 and 5 demonstrate that IP_3 signaling within sheath cells is required for their contractile activity.

Sheath Cell IP_3 Is Generated by Phospholipase C (PLC)-γ

IP_3 is generated by PLC-mediated hydrolysis of the membrane lipid phosphatidylinositol 4,5-bisphosphate (PIP_2). Six predicted PLC-encoding genes are present in the *C. elegans* genome: *egl-8*, *plc-1*, *plc-2*, *plc-3*, *plc-4* and *pll-1*. Worms were fed PLC dsRNA beginning at the L1 larva stage (i.e., long-term feeding) to identify the PLC(s) that generate sheath cell IP_3. EGL-8, PLC-2, PLL-1, and PLC-4 RNAi worms had normal oocytes. Basal and ovulatory sheath contractions in

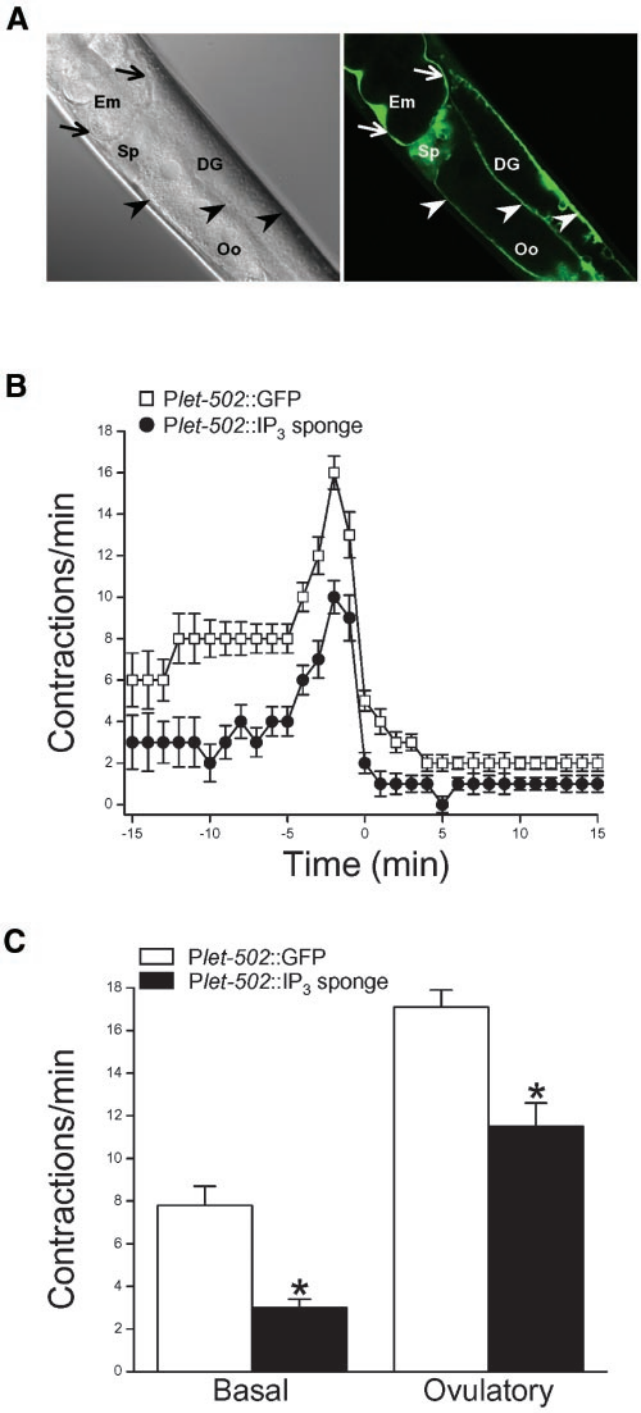

Figure 5. Effect of sheath cell IP_3 sponge expression on contractile activity. (A) P*let-502*::GFP expression pattern. Confocal differential interference contrast micrograph (left) and corresponding GFP fluorescence micrograph (right). GFP is expressed in proximal and distal gonad sheath cells (arrowheads), the spermatheca (Sp), and uterine sheath cells (arrows). DG, distal gonad; Em, embryo; Oo, oocyte. (B) Rates of sheath contraction during a single ovulatory cycle in control worms expressing P*let-502*::GFP and P*let-502*::IP_3 sponge. Values are means ± SE (n = 15–19). *C.* Basal and peak ovulatory contraction rates in control and IP_3 sponge-expressing worms. Values are means ± SE (n = 12–19). *$p < 0.0002$ compared with control worms expressing P*let-502*::GFP.

these worms were not significantly ($p > 0.06$) different from GFP RNAi control worms (our unpublished data).

PLC-1 and PLC-3 RNAi worms exhibited an emo phenotype, but otherwise had a largely normal appearance. In the majority of animals examined, the emo phenotype was severe and characterized by the presence of multiple emo oocytes in the gonad. *plc-3(RNAi)* worms were completely sterile. The brood size of *plc-1(RNAi)* animals was 12 ± 2 (n = 10), which was significantly ($p < 0.0001$) smaller than the brood size of 323 ± 18 (n = 10) observed in GFP RNAi control worms.

Because of the severe emo phenotype, we only characterized basal sheath contractions in *plc-1(RNAi)* and *plc-3(RNAi)* worms. As shown in Figure 6A, the rate of basal sheath contraction was reduced significantly ($p < 0.01$) from 7.3 to 2.1 contractions/min in worms fed *plc-3* dsRNA. In contrast, disruption of *plc-1* expression had no significant ($p > 0.05$) effect on basal sheath contractility.

To examine further the role of *plc-1* and *plc-3* in sheath contraction, we performed a short-term (i.e., 16–24 h) dsRNA feeding protocol in L4 larvae. Twenty percent of the *plc-1(RNAi)* worms (n = 30) exhibited an emo phenotype; oocytes in all other worms were normal in appearance. Rates of basal and peak ovulatory sheath contraction in *plc-1(RNAi)* worms with normal oocytes were 10.4 and 18.8 contractions/min, respectively, and were not significantly ($p > 0.05$) different from control worms fed GFP dsRNA (Figure 6B).

plc-1(RNAi) worms exhibited defects in spermatheca function. In two of the 14 worms examined, the maturing oocyte failed to enter the spermatheca, and in three of 14 worms fertilized oocytes failed to enter the uterus. We also observed a significant prolongation of forceful ovulatory contractions. Forceful ovulatory contractions lasted 1.7 ± 0.2 min (n = 11) in GFP RNAi control worms and 3.9 ± 0.7 min (n = 14; $p < 0.05$) in worms fed *plc-1* dsRNA. This prolongation of ovulatory contractions is likely due to defects in spermatheca function.

IP_3 signaling controls spermatheca dilation (Bui and Sternberg, 2002). We have observed that PLC-1::GFP is not expressed in sheath cells but expresses strongly in the spermatheca (our unpublished data). Failure of the spermatheca to dilate properly in *plc-1(RNAi)* worms would result in retention of the oocyte in the gonad with continued triggering of ovulatory contractions. Based on the results of both the long- and short-term dsRNA feeding experiments, we conclude that the emo and sterile phenotypes observed in worms fed *plc-1* dsRNA are due primarily to defects in spermatheca function.

Seventy-five percent of L4 worms fed *plc-3* dsRNA (n = 28) for 16–24 h exhibited an emo phenotype. Sheath contractility in *plc-3(RNAi)* worms with normal oocytes was reduced compared with control animals fed GFP dsRNA. Rates of basal and peak ovulatory contractions were reduced significantly from 9.6 to 6.6 contractions/min ($p < 0.05$) and from 17.8 to 13.2 contractions/min ($p < 0.01$), respectively (Figure 6B). Interestingly, we also observed that the time from the beginning of oocyte meiotic maturation until the start of forceful ovulatory contractions was increased significantly ($p < 0.05$) from 4.2 ± 0.5 min (n = 10) in control GFP RNAi worms to 9.1 ± 1.9 min (n = 8) in *plc-3(RNAi)* animals. This suggests that disruption of *plc-3* expression reduces the rate of IP_3 generation required for triggering ovulatory sheath contractions.

To determine whether *plc-3* is expressed in the sheath cells, we constructed a PLC-3 GFP translational reporter. As shown in Figure 6C, PLC-3::GFP is expressed in the sheath cells. Together with the results shown in Figure 6, we con-

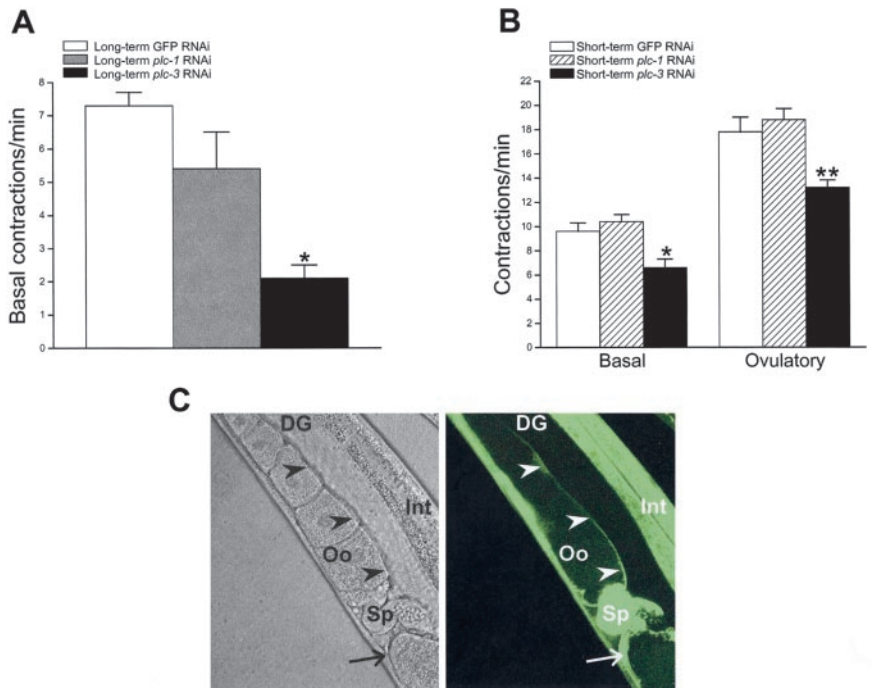

Figure 6. Effect of dsRNA-induced disruption of *plc-1* and *plc-3* expression on sheath contractility. (A) Rates of basal sheath contraction in adult worms fed GFP, *plc-1*, or *plc-3* dsRNA beginning at the L1 larval stage. Values are means ± SE (n = 7–29). *$p < 0.01$ compared with GFP dsRNA-fed worms. (B) Rates of basal and peak ovulatory sheath contractions in adult worms fed dsRNA for 16–24 h beginning in late-stage L4 larvae. Values are means ± SE (n = 8–13). *$p < 0.05$ and **$p < 0.01$ compared with GFP dsRNA-fed worms. (C) PLC-3::GFP expression pattern. Confocal differential interference contrast micrograph (left) and corresponding GFP fluorescence micrograph (right). GFP is expressed in proximal gonad sheath cells (arrowheads), spermatheca (Sp) and uterine sheath cells (arrow). DG, distal gonad; Int, intestine; Oo, oocyte.

clude that the predicted PLC-γ homolog encoded by *plc-3* is responsible for IP_3 generation that controls sheath cell contractile activity.

PLC-3::GFP is also expressed in the spermatheca. Consistent with this, we found that worms fed *plc-3* dsRNA exhibited defects in spermatheca function. Oocytes in four of 9 *plc-3(RNAi)* worms failed to complete entry into the spermatheca. Two of these oocytes were torn in half by premature closure of the gonad-spermatheca valve. Forceful ovulatory contractions also were prolonged from 1.7 ± 0.2 min (n = 11) to 5.3 ± 0.8 min (n = 8; $p < 0.01$) in *plc-3* RNAi animals compared with control worms fed GFP dsRNA.

Calcium Influx Is Required for Sheath Cell Contractions

The data presented above demonstrate that release of Ca^{2+} from IP_3-dependent intracellular stores triggers rhythmic sheath cell contraction under basal conditions and during ovulation. In many, but not all cell types, Ca^{2+} entry across the plasma membrane is required for generating and maintaining repetitive or oscillatory IP_3-dependent Ca^{2+} release (Shuttleworth, 1999; Sneyd *et al.*, 2004). To assess the role of Ca^{2+} influx on IP_3-dependent Ca^{2+} signaling in sheath cells, we characterized sheath contractile activity in isolated gonads where extracellular ionic composition could be controlled. As shown in Figure 7, removal of extracellular Ca^{2+} causes a rapid inhibition of sheath cell contractility. Calcium influx may be required to trigger Ca^{2+} release via IP_3 receptors, refill intracellular Ca^{2+} stores, and/or it may contribute to the overall pattern of intracellular Ca^{2+} increase needed for sheath cell contraction.

Ovulatory Sheath Contractions Are Triggered by LIN-3/LET-23 Signaling

MSP signaling through the VAB-1 Eph receptor tyrosine kinase triggers basal sheath contractions (Miller *et al.*, 2001). The primary signal that triggers ovulatory sheath contractions has not been described. However, signaling through the EGF-like ligand LIN-3 and the LET-23 tyrosine kinase receptor is required for spermathecal dilation during ovulation (Clandinin *et al.*, 1998; unpublished observations cited in McCarter *et al.*, 1999). We therefore tested the hypothesis that LIN-3/LET-23 signaling also controls ovulatory sheath contractions.

sy10 and *n1058* are reduction-of-function alleles of *let-23* (Aroian *et al.*, 1994) and *lin-3* (Ferguson and Horvitz, 1985), respectively. We examined sheath contractility in young adult *let-23(sy10)* and *lin-3(n1058)* worms. The gonads of these worms contained normal oocytes or one or two emo oocytes. The presence of one or two emo oocytes had no effect on contractile activity (our unpublished data).

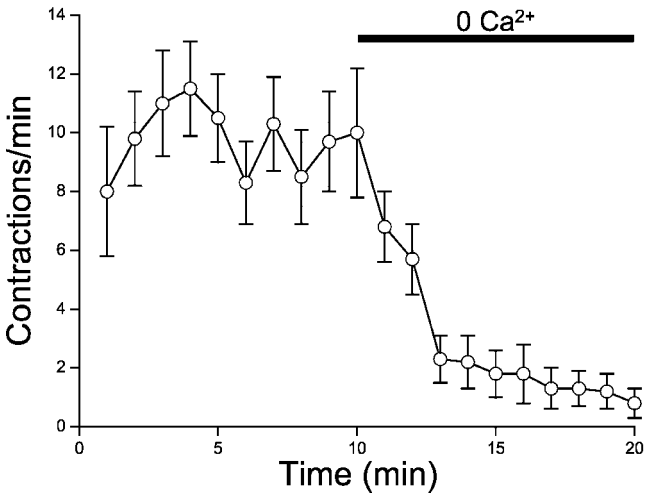

Figure 7. Effect of extracellular Ca^{2+} removal on sheath cell contractile activity in isolated gonads. Control bath solution containing 2 mM Ca^{2+} was replaced with a Ca^{2+}-free solution containing 1 mM EGTA. Values are means ± SE (n = 5–6).

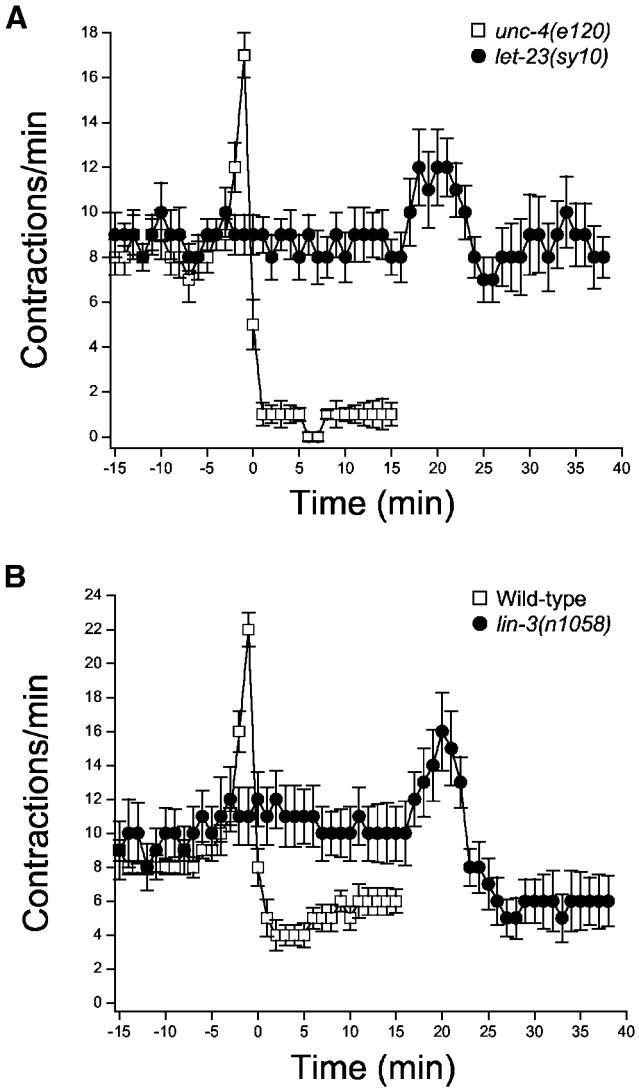

Figure 8. Rates of sheath contraction during a single ovulatory cycle in *let-23* (A) and *lin-3* (B) reduction-of-function mutants. Contractile activity was synchronized in control and mutant worms to the time ovulatory contractions were completed. Time 0 is defined as the time ovulation was complete in *unc-4(e120)* and wild-type control worms. Data for both groups of worms are plotted beginning 10 min before initiation of oocyte meiotic maturation. Values are means ± SE (n = 8–12).

Rates of basal sheath contraction in *let-23(sy10)* and *lin-3(n1058)* worms were not significantly ($p > 0.1$) different from those observed in control animals (Figure 8). Apparent ovulatory contractions were observed in both mutants, but no successful ovulations were detected. The lack of successful ovulations is most likely due to disruption of spermatheca contractile activity. *let-23(sy10)* and *lin-3(n1058)* worms showed defects in spermatheca function similar to those of *itr-1(sa73)* mutant discussed earlier.

The rate of contraction and sheath displacement increased in both *let-23(sy10)* and *lin-3(n1058)* worms after induction of oocyte meiotic maturation (Figure 8). The mean ± SE peak rate of contraction and displacement for *let-23(sy10)* worms were 14.6 ± 1.7 contractions/min (n = 8) and 4.6 ± 0.4 μm (n = 8) and were not significantly ($p > 0.2$) different from ovulatory contractions observed in *unc-4(e120)* control worms. In *lin-3(n1058)* worms, peak rate of contraction and displacement were 17.1 ± 2.1 contractions/min (n = 12) and 4.2 ± 0.2 μm (n = 12). Mean displacement was not significantly ($p > 0.7$) different from that observed in wild-type animals. However, the rate of ovulatory contraction was slightly but significantly ($p < 0.04$) lower than that in control worms.

For both *let-23(sy10)* and *lin-3(n1058)* worms, there was a striking and significant ($p < 0.0001$) delay in the initiation of ovulatory contractions. In *unc-4(e120)* control, wild-type control, *let-23(sy10)*, and *lin-3(n1058)* worms, ovulatory contractions were initiated 3.2 ± 0.2 (n = 9), 3.5 ± 0.3 (n = 10), 22.8 ± 1.0 (n = 8), and 23.0 ± 1.6 min (n = 12), respectively, after induction of meiotic maturation. Ovulatory contractions also were significantly ($p < 0.0001$) prolonged in *let-23(sy10)* and *lin-3(n1058)* worms (Figure 8), which is likely due to defects in spermatheca function and retention of oocytes in the gonad.

LIN-3/LET-23, MSP/VAB-1, and PLC-3 Regulate ITR-1

Data in Figures 1–8 indicate that sheath contractions are regulated by LIN-3/LET-23 and MSP/VAB-1 signaling through PLC-3 to ITR-1. We performed epistasis analysis to define this putative signaling pathway more directly. Specifically, we fed *itr-1(sy327)* worms *let-23*, *vab-1*, or *plc-3* dsRNA beginning at the L1 larval stage (i.e., long-term feeding) to determine if a gain-of-function mutation in ITR-1 would suppress the defects in sheath contraction induced by RNAi of these genes.

unc-24(e138) control worms fed GFP dsRNA showed normal cycles of basal and ovulatory sheath contractions (our unpublished data). *plc-3(RNAi)* significantly ($p < 0.001$) reduced the mean ± SE rate of basal sheath contraction to 2.3 ± 0.9 contractions/min (n = 7) and completely inhibited ovulatory contractions (Figure 9A). Sheath contractile activity of *itr-1(sy327)* worms fed GFP dsRNA worms was similar to that of unfed animals described above (compare Figures 2A and 9A); rates of basal sheath contraction were elevated compared with control animals and contraction rate declined during ovulation.

The inhibitory effect of *plc-3(RNAi)* on basal sheath contraction was suppressed completely by *itr-1(sy327)* (Figure 9A). In addition, *itr-1(sy327);plc-3(RNAi)* worms showed near-normal ovulatory contractions. During ovulation, the mean ± SE rate of peak sheath contraction increased significantly ($p < 0.006$) from 10.8 ± 0.6 (n = 5) to 16.0 ± 1.2 contractions/min (n = 6) and then declined steadily (Figure 9A).

MSP signaling occurs through VAB-1, an Eph receptor tyrosine kinase (Miller *et al.*, 2001). *vab-1(RNAi)* inhibited basal sheath contractility significantly ($p < 0.001$) from a mean value of 8.8 to 4.8 contractions/min (Figure 9B). These findings are similar to those of Miller *et al.* (2001). *itr-1(sy327)* suppressed completely the inhibitory effect of *vab-1(RNAi)* (Figure 9B). Mean rate of basal sheath contraction in *itr-1(sy327);vab-1(RNAi)* worms was 11.3, which is significantly ($p < 0.0001$) greater than that observed in *unc-24(e138);vab-1(RNAi)* control animals (Figure 9B).

Worms fed *let-23* (Figure 9C) or *lin-3* (our unpublished data) dsRNA were sterile and exhibited sheath contractile activity similar to that observed with *let-23(sy10)* and *lin-3(n1058)* mutants (compare Figures 8 and 9C). The major effect of *let-23(RNAi)* was a small but significant ($p < 0.007$) reduction of the peak rate of contraction from a mean ± SE value of 19.0 ± 1.4 (n = 5) to 13.8 ± 0.7 (n = 6) contractions/min, and a highly significant ($p < 0.0001$) delay in the onset of ovulatory contractions (Figure 9C). In *unc-24(e138);*GFP RNAi control and *unc-24(e138);let-23(RNAi)* worms the

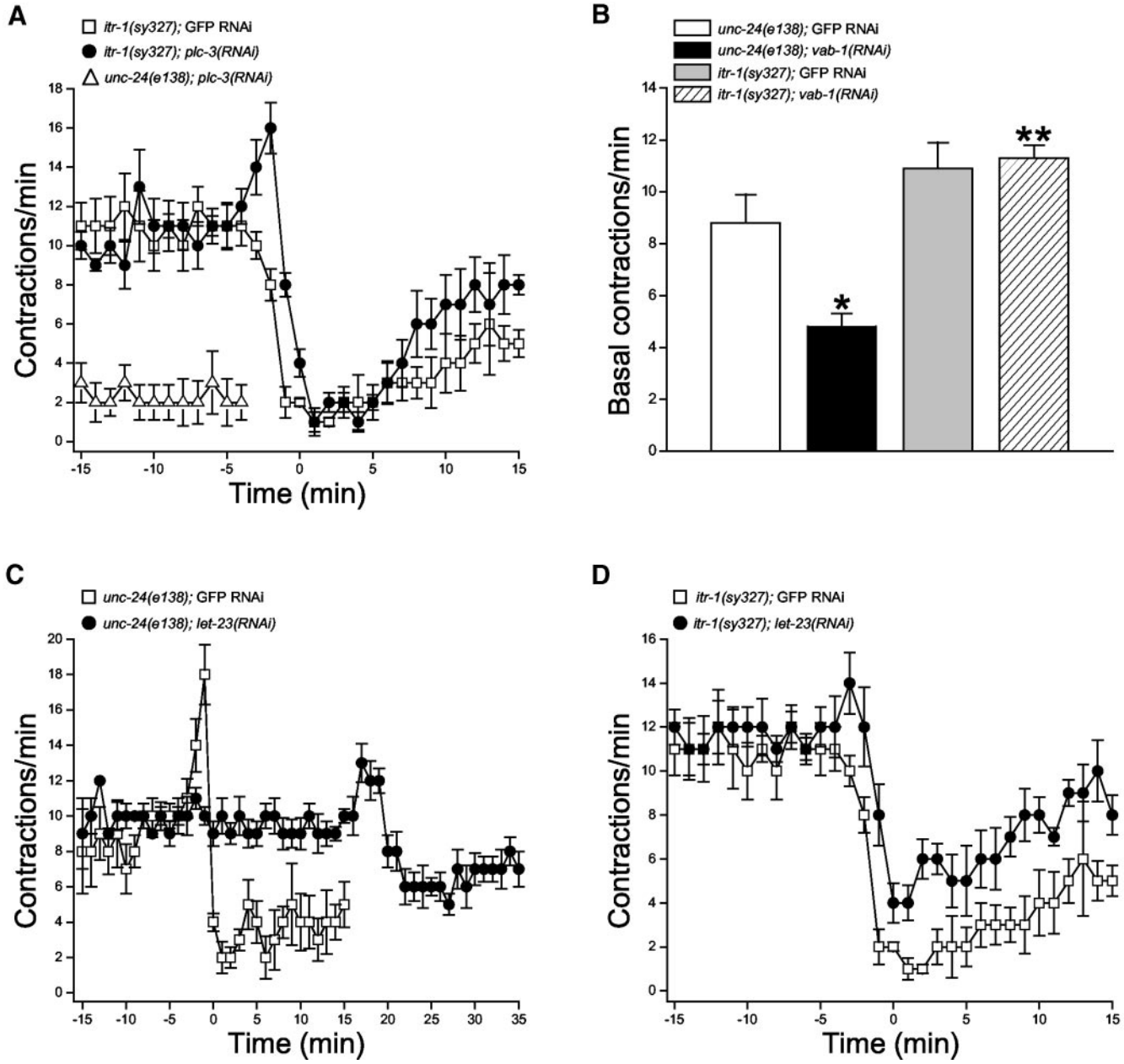

Figure 9. Effects of the *itr-1(sy327)* gain-of-function mutation on RNAi-induced knockdown of PLC-3, VAB-1 and LET-23 expression. (A) Rates of sheath contraction in *unc-24(e138)* control worms fed *plc-3* dsRNA and *itr-1(sy327)* mutants fed *plc-3* or GFP dsRNA. No ovulatory contractions were observed in *unc-24(e138);plc-3(RNAi)* worms. Values are means ± SE (n = 5–7). (B) Rates of basal sheath contraction in *unc-24(e138)* control worms and *itr-1(sy327)* mutants fed GFP or *vab-1* dsRNA. Values are means ± SE (n = 5–7). *$p < 0.007$ compared with *unc-24(e138);*GFP RNAi worms. **$p < 0.0001$ compared with *unc-24(e138);vab-1(RNAi)* worms. (C) Rates of sheath contraction in *unc-24(e138)* control worms fed GFP or *let-23* dsRNA. Contractile activity was synchronized to the time ovulatory contractions were completed. Time 0 is defined as the time ovulation was complete in *unc-4(e120)* GFP RNAi control worms. Data for both groups of worms are plotted beginning 10 min before initiation of oocyte meiotic maturation. Values are means ± SE (n = 5–6). (D) Rates of sheath contraction in *itr-1(sy327)* mutant worms fed GFP or *let-23* dsRNA. Values are means ± SE (n = 5).

mean ± SE time from initiation of meiotic maturation until completion of ovulation was 4.0 ± 0.5 (n = 6) and 24.3 ± 1.1 min (n = 6), respectively. *itr-1(sy327)* suppressed the delay in initiation of ovulatory contractions induced by *let-23(RNAi)* (Figure 9D). The mean ± SE time from initiation of meiotic maturation until completion of ovulation was 4.2 ± 0.4 min (n = 5) in *itr-1(sy327);*GFP RNAi worms and 4.6 ± 0.2 min (n = 5) in *itr-1(sy327);let-23(RNAi)* animals. These values were not significantly ($p > 0.4$) different.

Together, the data in Figure 9 demonstrate that LIN-3/LET-23 and MSP/VAB-1 signaling regulate sheath contraction via activation of ITR-1. The results also demonstrate that ITR-1 is activated by PLC-3-generated IP_3. As discussed above, a screen of all six predicted *C. elegans* PLC-encoding genes demonstrated that PLC-3, a predicted PLC-γ homolog, is the only PLC responsible for regulation of sheath contraction. We conclude therefore that LIN-3/LET-23 and

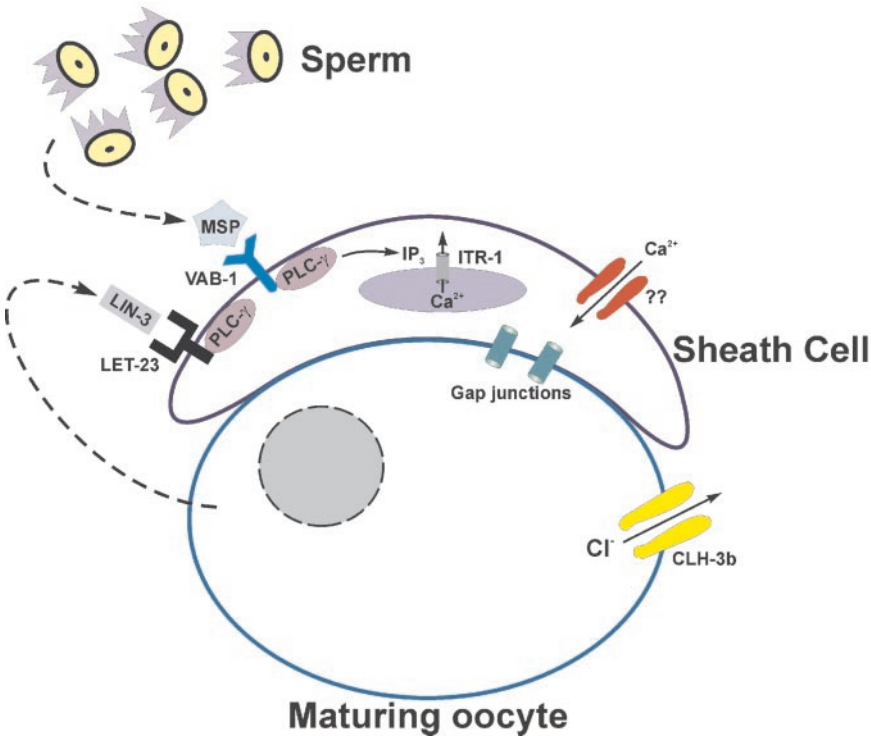

Figure 10. Summary of signaling events know to regulate sheath cell contraction. MSP is secreted by sperm and induces basal sheath contractions by binding to VAB-1 (Miller *et al.*, 2001) and activating PLC-γ. LIN-3 is secreted by the maturing oocyte and triggers ovulatory sheath contractions. Activation of the ClC anion channel CLH-3b during oocyte meiotic maturation (Denton *et al.*, 2003) may depolarize the gap junction coupled sheath cells and inhibit Ca^{2+} entry required for regulating IP_3-dependent Ca^{2+} oscillations and/or refilling intracellular stores.

MSP/VAB-1 signaling activates PLC-3 leading to the generation of IP_3 and subsequent activation of ITR-1.

DISCUSSION

Figure 10 summarizes the signaling events that regulate sheath cell contractility. We have demonstrated here that Ca^{2+} release from intracellular stores via the IP_3R ITR-1 is required for rhythmic sheath contraction under basal conditions and during ovulation (Figures 1–3). Ovulatory sheath contractions and spermatheca dilation are triggered by oocytes undergoing meiotic maturation (McCarter *et al.*, 1999). *emo-1* encodes a homologue of the Sec61 γ subunit, which plays a role in the translocation of secretory and membrane proteins into the endoplasmic reticulum (Iwasaki *et al.*, 1996). Spermatheca function and ovulatory sheath contractions are abnormal in *emo-1* mutants, suggesting that a factor secreted from maturing oocytes controls sheath cell and spermatheca function (Iwasaki *et al.*, 1996). Sternberg and coworkers have demonstrated that IP_3 signaling through LIN-3/LET-23 controls spermatheca dilation (Clandinin *et al.*, 1998; Bui and Sternberg, 2002), indicating that LIN-3 is the regulatory signal secreted from maturing oocytes.

LET-23 is expressed in sheath cells (Sternberg, personal communication) and *lin-3* and *let-23* reduction-of-function mutants exhibit defects in ovulatory sheath contractile activity (Figures 8). The most striking defect is seven- to eight-fold increase in the time ovulatory contractions are initiated after meiotic maturation has begun. This delay likely reflects reduced activity of LIN-3 and LET-23. For example, the *let-23(sy10)* allele is a C368Y mutation (Aroian *et al.*, 1994). This mutation is located at the interface of cysteine-rich domain #1 and ligand-binding domain #2 and may disrupt ligand binding and/or receptor dimerization required for activation and signal transduction (Garrett *et al.*, 2002). Consistent with this interpretation, knockdown of *let-23* expression by RNAi induced a sheath contraction phenotype similar to that of the reduction-of-function mutation (Figure 9C).

LET-23 and VAB-1 are predicted receptor tyrosine kinases. Receptor tyrosine kinases trigger intracellular signaling events in part by activating PLC-γ (Rhee, 2001). We demonstrated that PLC-3, a PLC-γ homolog, is expressed in sheath cells and the spermatheca and regulates the ovulatory functions of these tissues (Figure 6). Interestingly, we also observed that PLC-1, a predicted PLC-ε homolog, is expressed in the spermatheca (Baylis, unpublished observations) and regulates spermatheca dilation. PLC-ε is regulated by Ras and Rho GTPases and by $G\alpha_{12/13}$ and $G\beta\gamma$ G proteins (Rhee, 2001; Wing *et al.*, 2003). A number of studies suggest that LIN-3/LET-23 signaling in the gonad is Ras-independent (for review, see (Clandinin *et al.*, 1998). Thus, PLC-ε activation in the spermatheca is likely mediated through LIN-3/LET-23 independent signaling mechanisms. An intriguing possibility is that PLC-ε is activated by mechanical force, which has been proposed to activate G protein signaling in other cell types (Aikawa *et al.*, 1999; Bornfeldt, 2000; Kawamura *et al.*, 2003).

Although we have not measured sheath cell Ca^{2+} directly, it is likely that cytoplasmic Ca^{2+} concentration oscillates and peaks before each sheath cell contraction. Oscillating Ca^{2+} signals have been observed in innumerable cell types and are due to repetitive release of Ca^{2+} from intracellular stores followed by store reuptake and plasma membrane extrusion via Ca^{2+} transporters (Berridge *et al.*, 2000, 2003). Repetitive Ca^{2+} release is thought to arise from oscillating IP_3 levels and/or Ca^{2+}-induced Ca^{2+} release (CICR) (Hirose *et al.*, 1999; Berridge *et al.*, 2000, 2003; Nash *et al.*, 2001). CICR is a self-propagating process. As Ca^{2+} leaves the stores through an IP_3R, it feeds back on the channel and activates it further. Elevation of local Ca^{2+} levels activates neighboring IP_3Rs, leading ultimately to a rise in cytoplasmic Ca^{2+}. High concen-

trations of Ca^{2+} in turn feedback and inhibit IP_3Rs, allowing cytoplasmic Ca^{2+} levels to fall as the ion is extruded from the cell and pumped back into intracellular stores.

The precise role of plasma membrane Ca^{2+} entry in generating and maintaining cytoplasmic Ca^{2+} oscillations is unclear. Calcium oscillations in some cell types continue for long periods in the absence of extracellular Ca^{2+} (Lechleiter and Clapham, 1992). In contrast, oscillatory Ca^{2+} signals in other cell types are strictly dependent on Ca^{2+} influx (Shuttleworth, 1999; Shuttleworth and Mignen, 2003). Plasma membrane Ca^{2+} entry likely provides a Ca^{2+} source for refilling intracellular stores and also may control the frequency, amplitude, and duration of Ca^{2+} oscillations as well as rates of intracellular Ca^{2+} change (Zhao *et al*., 1990; Shuttleworth and Mignen, 2003). Shuttleworth (Shuttleworth and Mignen, 2003; Sneyd *et al*., 2004) has argued that the rate of plasma membrane Ca^{2+} entry, even in cells where oscillations continue in the absence of external Ca^{2+}, modulates the frequency of oscillations by triggering CICR via IP_3Rs.

Figure 7 demonstrates that plasma membrane Ca^{2+} influx is required for maintaining sheath contractions. Calcium influx into nonexcitable cells such as blood cells and endothelial and epithelial cells occurs primarily by voltage-independent receptor-, second messenger-, and store-operated Ca^{2+} channels (ROCCs, SMOCCs, and SOCCs) (Elliott, 2001; Zitt *et al*., 2002). Gating of these channels is not regulated strongly by membrane voltage. However, membrane depolarization reduces Ca^{2+} influx through ROCCs, SMOCCs, and SOCCs by reducing the electrical gradient driving Ca^{2+} entry. In many cell types, Cl^- channels play important roles in modulating membrane potential, thereby regulating Ca^{2+} influx and cytoplasmic Ca^{2+} levels (Ono *et al*., 1998; Mair *et al*., 1998; McLarnon *et al*., 2000).

The findings of the present study support our hypothesis on the role of CLH-3b in intercellular communication processes that regulate sheath cell contractile activity. As discussed above, CLH-3b is activated during oocyte meiotic maturation and functions to delay the onset of sheath cell ovulatory contractions (Rutledge *et al*., 2001; Strange, 2003). We have proposed that this delay is brought about by CLH-3b-mediated depolarization of gap junction-coupled sheath cells and that this in turn inhibits Ca^{2+} entry required for IP_3-regulated cytoplasmic Ca^{2+} oscillations (Rutledge *et al*., 2001; Strange, 2003). Our studies demonstrate clearly that basal and ovulatory sheath contractions are regulated by IP_3 signaling and plasma membrane Ca^{2+} influx. In addition, we have observed that oocytes are depolarized during meiotic maturation (Boehmer and Strange, unpublished observations). Two important questions remain to be answered. Does activation of CLH-3b in the oocyte depolarize sheath cells, and what events override the inhibitory action of the channel to trigger sheath ovulatory contractions later in the meiotic maturation cycle? It also will be important to determine the molecular identity of the sheath cell Ca^{2+} influx pathway and the mechanisms by which it is regulated.

ACKNOWLEDGMENTS

We thank Todd Lamitina for critically reading the manuscript. Strains used in this work were provided by the *Caenorhabditis* Genetics Center (University of Minnesota, Minneapolis, MN).This work was supported by National Institutes of Health grants R01 DK61168 and P01 DK58212 to K.S. and by Medical Research Council Senior NonClinical Fellowship G117/466 to H.A.B.

REFERENCES

Aikawa, R., Komuro, I., Yamazaki, T., Zou, Y., Kudoh, S., Zhu, W., Kadowaki, T., and Yazaki, Y. (1999). Rho family small G proteins play critical roles in mechanical stress-induced hypertrophic responses in cardiac myocytes. Circ. Res. *84*, 458–466.

Aroian, R.V., Lesa, G.M., and Sternberg, P.W. (1994). Mutations in the *Caenorhabditis elegans let-23* EGFR-like gene define elements important for cell-type specificity and function. EMBO J. *13*, 360–366.

Baylis, H.A., Furuichi, T., Yoshikawa, F., Mikoshiba, K., and Sattelle, D.B. (1999). Inositol 1,4,5-trisphosphate receptors are strongly expressed in the nervous system, pharynx, intestine, gonad and excretory cell of *Caenorhabditis elegans* and are encoded by a single gene (*itr-1*). J. Mol. Biol. *294*, 467–476.

Berridge, M.J., Bootman, M.D., and Roderick, H.L. (2003). Calcium signalling: dynamics, homeostasis and remodelling. Nat. Rev. Mol. Cell. Biol. *4*, 517–529.

Berridge, M.J., Lipp, P., and Bootman, M.D. (2000). The versatility and universality of calcium signalling. Nat. Rev. Mol. Cell. Biol. *1*, 11–21.

Bornfeldt, K.E. (2000). Stressing Rac, Ras, and downstream heat shock protein 70. Circ. Res. *86*, 1101–1103.

Brenner, S. (1974). The genetics of *Caenorhabditis elegans*. Genetics *77*, 71–94.

Bui, Y.K., and Sternberg, P.W. (2002). *Caenorhabditis elegans* inositol 5-phosphatase homolog negatively regulates inositol 1,4,5-triphosphate signaling in ovulation. Mol. Biol. Cell *13*, 1641–1651.

Cheng, C.Y., and Mruk, D.D. (2002). Cell junction dynamics in the testis: Sertoli-germ cell interactions and male contraceptive development. Physiol. Rev. *82*, 825–874.

Clandinin, T.R., DeModena, J.A., and Sternberg, P.W. (1998). Inositol trisphosphate mediates a RAS-independent response to LET-23 receptor tyrosine kinase activation in *C. elegans*. Cell *92*, 523–533.

Dal Santo, P., Logan, M.A., Chisholm, A.D., and Jorgensen, E.M. (1999). The inositol trisphosphate receptor regulates a 50-second behavioral rhythm in *C. elegans*. Cell *98*, 757–767.

Denton, J., Nehrke, K., Rutledge, E., Morrison, R., and Strange, K. (2003). Alternative splicing of N- and C-termini of a *C. elegans* ClC channel alters gating and sensitivity to external Cl^- and H^+. J. Physiol. *555*, 97–114.

Elliott, A.C. (2001). Recent developments in non-excitable cell calcium entry. Cell Calcium *30*, 73–93.

Eppig, J.J. (2001). Oocyte control of ovarian follicular development and function in mammals. Reproduction *122*, 829–838.

Ferguson, E.L., and Horvitz, H.R. (1985). Identification and characterization of 22 genes that affect the vulval cell lineages of the nematode *Caenorhabditis elegans*. Genetics *110*, 17–72.

Garrett, T.P., *et al*. (2002). Crystal structure of a truncated epidermal growth factor receptor extracellular domain bound to transforming growth factor α. Cell *110*, 763–773.

Hall, D.H., Winfrey, V.P., Blaeuer, G., Hoffman, L.H., Furuta, T., Rose, K.L., Hobert, O., and Greenstein, D. (1999). Ultrastructural features of the adult hermaphrodite gonad of *Caenorhabditis elegans*: relations between the germ line and soma. Dev. Biol. *212*, 101–123.

Hirose, K., Kadowaki, S., Tanabe, M., Takeshima, H., and Iino, M. (1999). Spatiotemporal dynamics of inositol 1,4,5-trisphosphate that underlies complex Ca^{2+} mobilization patterns. Science *284*, 1527–1530.

Hobert, O. (2002). PCR fusion-based approach to create reporter gene constructs for expression analysis in transgenic *C. elegans*. Biotechniques *32*, 728–730.

Hubbard, E.J., and Greenstein, D. (2000). The *Caenorhabditis elegans* gonad: a test tube for cell and developmental biology. Dev. Dyn. *218*, 2–22.

Iwasaki, K., Liu, D.W., and Thomas, J.H. (1995). Genes that control a temperature-compensated ultradian clock in *Caenorhabditis elegans*. Proc. Natl. Acad. Sci. USA *92*, 10317–10321.

Iwasaki, K., McCarter, J., Francis, R., and Schedl, T. (1996). emo-1, a *Caenorhabditis elegans* Sec61p γ homologue, is required for oocyte development and ovulation. J. Cell Biol. *134*, 699–714.

Kamath, R.S., Martinez-Campos, M., Zipperlen, P., Fraser, A.G., and Ahringer, J. (2000). Effectiveness of specific RNA-mediated interference through ingested double-stranded RNA in *Caenorhabditis elegans*. Genome Biol. *2*, 2.1–2.10.

Kanematsu, T., Misumi, Y., Watanabe, Y., Ozaki, S., Koga, T., Iwanaga, S., Ikehara, Y., and Hirata, M. (1996). A new inositol 1,4,5-trisphosphate binding protein similar to phospholipase C-δ_1. Biochem. J. *313*, 319–325.

Kawamura, S., Miyamoto, S., and Brown, J.H. (2003). Initiation and transduction of stretch-induced RhoA and Rac1 activation through caveolae: cytoskeletal regulation of ERK translocation. J. Biol. Chem. *278*, 31111–31117.

Kelly, W.G., and Fire, A. (1998). Chromatin silencing and the maintenance of a functional germline in *Caenorhabditis elegans.* Development *125*, 2451–2456.

Lechleiter, J.D., and Clapham, D.E. (1992). Molecular mechanisms of intracellular calcium excitability in *X. laevis* oocytes. Cell *69*, 283–294.

Mair, N., Frick, M., Meraner, A., Schramek, H., and Dietl, P. (1998). Long-term induction of a unique $C1^-$ current by endothelin-1 in an epithelial cell line from rat lung: evidence for regulation of cytoplasmic calcium. J. Physiol. *511*, 55–65.

Matzuk, M.M., Burns, K.H., Viveiros, M.M., and Eppig, J.J. (2002). Intercellular communication in the mammalian ovary: oocytes carry the conversation. Science *296*, 2178–2180.

McCarter, J., Bartlett, B., Dang, T., and Schedl, T. (1999). On the control of oocyte meiotic maturation and ovulation in *Caenorhabditis elegans.* Dev. Biol. *205*, 111–128.

McLarnon, J.G., Helm, J., Goghari, V., Franciosi, S., Choi, H.B., Nagai, A., and Kim, S.U. (2000). Anion channels modulate store-operated calcium influx in human microglia. Cell Calcium *28*, 261–268.

Mello, C.C., Kramer, J.M., Stinchcomb, D., and Ambros, V. (1991). Efficient gene transfer in *C. elegans*: extrachromosomal maintenance and integration of transforming sequences. EMBO J. *10*, 3959–3970.

Miller, M.A., Nguyen, V.Q., Lee, M.H., Kosinski, M., Schedl, T., Caprioli, R.M., and Greenstein, D. (2001). A sperm cytoskeletal protein that signals oocyte meiotic maturation and ovulation. Science *291*, 2144–2147.

Nash, M.S., Young, K.W., Challiss, R.A., and Nahorski, S.R. (2001). Intracellular signalling. Receptor-specific messenger oscillations. Nature *413*, 381–382.

Nehrke, K., Begenisich, T., Pilato, J., and Melvin, J.E. (2000). *C. elegans* ClC-type chloride channels: novel variants and functional expression. Am. J. Physiol. *279*, C2052–C2066.

Ono, K., Nakao, M., and Iijima, T. (1998). Chloride-sensitive nature of the histamine-induced Ca2+ entry in cultured human aortic endothelial cells. J. Physiol. *511*, 837–849.

Otsuki, M., Fukami, K., Kohno, T., Yokota, J., and Takenawa, T. (1999). Identification and characterization of a new phospholipase C-like protein, $PLC\text{-}L_2$. Biochem. Biophys. Res. Commun. *266*, 97–103.

Rhee, S.G. (2001). Regulation of phosphoinositide-specific phospholipase C. Annu. Rev. Biochem. *70*, 281–312.

Rutledge, E., Bianchi, L., Christensen, M., Boehmer, C., Morrison, R., Broslat, A., Beld, A.M., George, A., Greenstein, D., and Strange, K. (2001). CLH-3, a ClC-2 anion channel ortholog activated during meiotic maturation in *C. elegans* oocytes. Curr. Biol. *11*, 161–170.

Rutledge, E., Denton, J., and Strange, K. (2002). Cell cycle- and swelling-induced activation of a *C. elegans* ClC channel is mediated by CeGLC-7α/β phosphatases. J. Cell Biol. *158*, 435–444.

Schriever, A.M., Friedrich, T., Pusch, M., and Jentsch, T.J. (1999). CLC chloride channels in *Caenorhabditis elegans.* J. Biol. Chem. *274*, 34238–34244.

Shuttleworth, T.J. (1999). What drives calcium entry during $[Ca^{2+}]_i$ oscillations?–challenging the capacitative model. Cell Calcium *25*, 237–246.

Shuttleworth, T.J., and Mignen, O. (2003). Calcium entry and the control of calcium oscillations. Biochem. Soc. Trans. *31*, 916–919.

Sijen, T., Fleenor, J., Simmer, F., Thijssen, K.L., Parrish, S., Timmons, L., Plasterk, R.H., and Fire, A. (2001). On the role of RNA amplification in dsRNA-triggered gene silencing. Cell *107*, 465–476.

Sneyd, J., Tsaneva-Atanasova, K., Yule, D.I., Thompson, J.L., and Shuttleworth, T.J. (2004). Control of calcium oscillations by membrane fluxes. Proc. Natl. Acad. Sci. USA *101*, 1392–1396.

Strange, K. (2003). From genes to integrative physiology: ion channel and transporter biology in *Caenorhabditis elegans.* Physiol. Rev. *83*, 377–415.

Walker, D.S., Gower, N.J., Ly, S., Bradley, G.L., and Baylis, H.A. (2002). Regulated disruption of inositol 1,4,5-trisphosphate signaling in *Caenorhabditis elegans* reveals new functions in feeding and embryogenesis. Mol. Biol. Cell *13*, 1329–1337.

Wing, M.R., Snyder, J.T., Sondek, J., and Harden, T.K. (2003). Direct activation of phospholipase C-ϵ by Rho. J. Biol. Chem. *278*, 41253–41258.

Zhao, H., Loessberg, P.A., Sachs, G., and Muallem, S. (1990). Regulation of intracellular Ca^{2+} oscillation in AR42J cells. J. Biol. Chem. *265*, 20856–20862.

Zitt, C., Halaszovich, C.R., and Luckhoff, A. (2002). The TRP family of cation channels: probing and advancing the concepts on receptor-activated calcium entry. Prog. Neurobiol. *66*, 243–264.